Uppsala University

Advanced Physics - Project Course

Course code: 1FA566

Probing odd-frequency superconductivity via thermoelectricity in a ferromagnet-superconductor junction

---

Author:
Kauê Rodrigues Alves

Supervisors:
Annica Black-Schaffer
Paramita Dutta

September 3, 2019

Contents

1 Abstract

This report aims to investigate the presence of odd-frequency superconductivity in the boundary of a ferromagnet-superconductor junction by looking at its effect over the Seebeck coefficient and the figure of merit across the junction. The thermoelectric coefficients are calculated using a scattering matrix approach [4]. It is shown that near the half-metallic limit, spin-singlet superconductivity is suppressed, and in the presence of a low Rashba spin-orbit interaction, the odd-frequency pairing amplitude dominates over the singlet pairing induced, being associated with the spin-flip Andreev reflection, a scattering process that forms odd-frequency pairings near the junction. In this regime, there is an enhancement in the Seebeck coefficient and thermoelectric figure of merit. We predict that the enhancement of the thermoelectricity is due to the odd-frequency pairing state. This happens as the major contribution is due to the sub-gap regime, where Andreev reflection is the possible phenomena to occur at the interface, and it is associated with the cooper pair injection within the superconductor. Thus odd-frequency superconductivity based heterostructures may be a good thermoelectrics.

2 Introduction

The superconducting state of most low-temperature superconductors can be well understood by means of the BCS Hamiltonian. The BCS theory [2] assumes that there is an effective attractive force between electrons (mediated by interactions with the lattice), that is responsible to condense the electrons in Cooper pairs, which in turn gives raise to superconductivity. The superconducting state can be characterized by the so-called *anomalous Green's function* $\mathcal{F}_{\alpha,\beta}(\vec{r},t) = \langle \mathcal{T}\psi_\alpha(\vec{r},t)\psi_\beta(0,0)\rangle$, where $\psi_\alpha(\vec{r},t)$ is the annihilation operator of an electron with spin α, at position $\vec{r}$ and time t, and $\mathcal{T}$ is the time-ordering operator. $\mathcal{F}_{\alpha,\beta}(\vec{r},t)$ can be regarded as the *pairing amplitude* of Cooper pairs. In conventional superconductors (those who can be fully understood by BCS theory), the pairing amplitude satisfy $T\mathcal{F}_{\alpha,\beta} = \mathcal{F}_{\alpha,\beta}$, where T is the time reversal operator. Nevertheless, it is also possible to have superconducting states whose pairing amplitude satisfies $T\mathcal{F}_{\alpha,\beta} = -\mathcal{F}_{\alpha,\beta}$. These are called *odd-frequency states* [3] [10]. They are expected to appear in certain hybrid structures [5], as the consequence of a proximity effect, even when conventional superconductivity is the leading phenomena [11], and the presence of odd-frequency superconductivity in a junction may have an impact over its thermoelectric coefficients [8]. Here we investigate the appearance of odd-frequency states in a ferromagnet-superconductor (FS) junction, and study its effect on the Seebeck coefficient and the figure of merit across the junction.

2.1 Thermoelectricity

Heat conduction and electrical conduction are both transport processes, and can interfere with each other: that is, a potential gradient can generate a heat current I_q and a temperature gradient can generate an electric current I_e (see figures 1, 2).

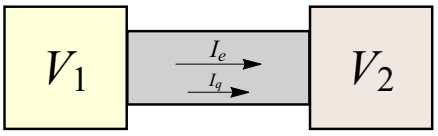

Figure 1: A heat current I_q being generated by a voltage difference.

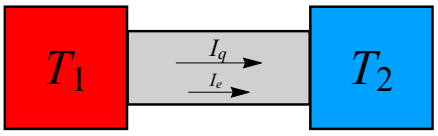

Figure 2: An electric current I_e being generated by a temperature difference.

In the linear regime, the relations between the currents I_e, I_q, the voltage V and the temperature difference ΔT can be written in a matrix form, and those relations are known as the *Onsager matrix equations*[12]

$$\begin{pmatrix} I_e \\ I_q \end{pmatrix} = \begin{pmatrix} L_{11} & L_{12} \\ L_{21} & L_{22}T \end{pmatrix} \begin{pmatrix} V \\ \Delta T/T \end{pmatrix}. \tag{1}$$

The L_{11} coefficient is the electric conductance G, and the L_{22} coefficient is the thermal conductance κ. It can be shown [12][13] that, under very general assumptions, the coefficients L_{12} and L_{21}, that mix electric and heat transport, are in fact equal, and they are usually referred to as the *thermoelectric coefficient* α. With those coefficients, eq. (1) reads

$$\begin{pmatrix} I_e \\ I_q \end{pmatrix} = \begin{pmatrix} G & \alpha \\ \alpha & \kappa T \end{pmatrix} \begin{pmatrix} V \\ \Delta T/T \end{pmatrix}. \tag{2}$$

From G, κ and α, we can define the *Seebeck coefficient* S

$$S = -\frac{1}{T}\frac{\alpha}{G}, \tag{3}$$

and the *thermoelectric figure of merit* zT [9]

$$zT = \frac{S^2 G T}{\kappa + \alpha S}. \tag{4}$$

The Seebeck coefficient provides the voltage generated due to a temperature difference, whereas the figure of merit is related to the efficiency of a thermoelectric device.

2.2 Thermoelectric coefficients in a junction

Consider a junction on which a bias V and a temperature difference δT are applied. Then, as a consequence, the Fermi functions of both sides of the junction will be different. Such a difference will generate a flux of particles, as particles from one side will tend to occupy less energetic states on the other side (see figure 3).

Assuming a linear regime, where the Fermi function $f(E + eV, T + \delta T/2)$ can be well-approximated by its Taylor expansion

$$f(E + eV, T + \delta T/2) \simeq f(E, T) + eV\frac{\partial f}{\partial E} + \frac{\delta T}{2}\frac{\partial f}{\partial T}, \tag{5}$$

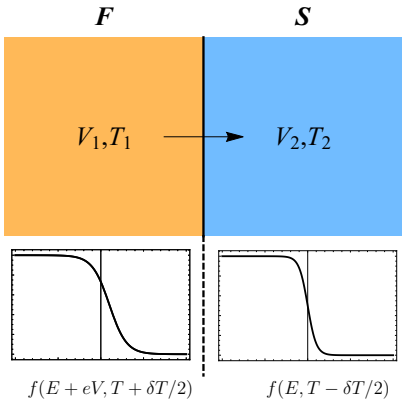

Figure 3: Representation of the flux generated by the mismatch of the Fermi functions between the two sides of a junction. E is energy, T is temperature and e is the electron charge.

the thermoelectric coefficients can be calculated, and are given by [4]

$$\begin{aligned} G &= \int \mathcal{T}(E) \left(-\frac{\partial f}{\partial E}\right) dE, \\ \alpha &= \int \mathcal{T}(E)(E-\mu) \left(-\frac{\partial f}{\partial E}\right) dE, \\ \kappa &= \frac{1}{T} \int \mathcal{T}(E)(E-\mu)^2 \left(-\frac{\partial f}{\partial E}\right) dE. \end{aligned} \tag{6}$$

where μ is the chemical potential and $\mathcal{T}(E)$ is the *transmission coefficient* of the junction.

2.3 Odd-frequency superconductivity

Superconducting states are characterized by the so-called *anomalous Green's function* (or pairing amplitude)

$$\mathcal{F}_{\alpha\beta}(x,t) = \langle \mathcal{T} \psi_\alpha(x,t) \psi_\beta(0,0) \rangle, \tag{7}$$

where $\mathcal{T}$ is the time-ordering operator. Due to the Fermi-Dirac statistics, the pairing amplitude must satisfy the following equality

$$SPT\mathcal{F}_{\alpha,\beta} = -\mathcal{F}_{\alpha,\beta}, \tag{8}$$

where S is the spin permutation operator, P is the parity operator, and T is the time-reversal operator, $S^2 = P^2 = T^2 = 1$. In the case of conventional superconductivity, which is described by BCS theory, the superconducting state is a spin singlet state with an even parity, called an s-wave state. Hence, its pairing function satisfies

$$S\mathcal{F}_{\alpha,\beta} = -\mathcal{F}_{\alpha,\beta}, \qquad P\mathcal{F}_{\alpha,\beta} = \mathcal{F}_{\alpha,\beta}, \qquad T\mathcal{F}_{\alpha,\beta} = \mathcal{F}_{\alpha,\beta}. \tag{9}$$

However, it is still possible for a superconducting state to satisfy $T\mathcal{F}_{\alpha,\beta} = -\mathcal{F}_{\alpha,\beta}$. Such states are called *odd-frequency states*. In order to preserve eq. (8), they must satisfy either

$$S\mathcal{F}_{\alpha,\beta} = -\mathcal{F}_{\alpha,\beta}, \qquad P\mathcal{F}_{\alpha,\beta} = -\mathcal{F}_{\alpha,\beta}, \tag{10}$$

or

$$S\mathcal{F}_{\alpha,\beta} = \mathcal{F}_{\alpha,\beta}, \qquad P\mathcal{F}_{\alpha,\beta} = \mathcal{F}_{\alpha,\beta}. \tag{11}$$

Here we look for states of the former case, which are even in both spin permutation and parity, as in a ferromagnet the polarization tends to align the spins, forming spin-triplet states.

The transmission coefficient has a contribution of both even and odd frequency parts of $\mathcal{F}$ [8]. It can be decomposed as

$$\mathcal{T}(E) \propto |\mathcal{F}_{even}(E) + \mathcal{F}_{odd}(E)|^2, \tag{12}$$

where the odd-frequency part is related to a reflection process known as spin-flip Andreev reflection. Thus, by increasing the odd-frequency states and decreasing the even-frequency states near the junction, one can alter the transmission coefficient, and therefore probe the odd-frequency superconductivity by looking at the thermoelectric coefficients. The increasing (decreasing) of odd (even)-frequency states will be done by changing the polarization of the ferromagnet and the strength of a spin-flip interface interaction called the Rashba interaction.

3 Model and theoretical formulation

3.1 Model

We consider a ferromagnet-superconductor junction as shown in figure 4. For $z < 0$, we have a ferromagnetic material, with magnetization $\vec{m} = (1, 0, 0)$, and exchange spin splitting Δ_{xc}. For $z > 0$, we have a superconductor, with a pairing potential Δ, which will be assumed to be constant.

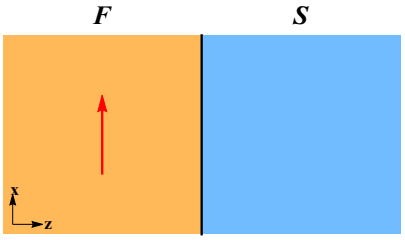

Figure 4: Representation of the FS junction. The red arrow shows the direction of magnetization inside the ferromagnet.

The Hamiltonian on the ferromagnet side of the junction is given by

$$\hat{H}_F = \int_{z<0} \left[\sum_\alpha \psi_\alpha^\dagger(\vec{r}) \left(-\frac{\hbar^2}{2m}\vec{\nabla}^2 - \frac{\Delta_{xc}}{2}\vec{m}\cdot\hat{\sigma} - \mu \right) \psi_\alpha(\vec{r}) \right] d\vec{r}, \tag{13}$$

where $\hat{\sigma}$ are the Pauli matrices. On the superconductor side, the Hamiltonian is given by

$$\hat{H}_S = \int_{z>0} \left[\sum_\alpha \psi_\alpha^\dagger(\vec{r}) \left(-\frac{\hbar^2}{2m}\vec{\nabla}^2 - \mu \right) \psi_\alpha(\vec{r}) + \left(\Delta\psi_\uparrow^\dagger(\vec{r})\psi_\downarrow^\dagger(\vec{r}) + H.c. \right) \right] d\vec{r}. \tag{14}$$

We also consider an interface interaction, at $z = 0$, given by

$$\hat{H}_{int} = \int \left[\sum_\alpha \psi_\alpha^\dagger(\vec{r})(Vd + \vec{\lambda}\cdot\hat{\sigma})\delta(z)\psi_\alpha(\vec{r}) \right] d\vec{r},$$

where V, d are respectively the height and width of the interface barrier and $\vec{\lambda} = \frac{\lambda}{\hbar}(P_y, -P_x, 0)$ is the Rashba field. The total Hamiltonian is expressed as

$$\hat{H} = \hat{H}_F + \hat{H}_S + \hat{H}_{int}. \tag{15}$$

3.2 BdG equations

In order to find the amplitudes of the excitations in the system, we assume that the Hamiltonian can be diagonalized by some fermionic operators γ_n,

$$\hat{H} = E_g + \sum_n \epsilon_n \gamma_n^\dagger \gamma_n \tag{16}$$

where E_g is the ground-state energy and the operators $\psi_\sigma(\vec{r})$ are related to γ_n by a unitary transformation

$$\begin{aligned} \psi_\uparrow(\vec{r}) &= \sum_n (u_{n\uparrow}(\vec{r})\gamma_n - v^*_{n\uparrow}(\vec{r})\gamma_n^\dagger) \\ \psi_\downarrow(\vec{r}) &= \sum_n (u_{n\downarrow}(\vec{r})\gamma_n + v^*_{n\downarrow}(\vec{r})\gamma_n^\dagger) \end{aligned} \tag{17}$$

From (16), we see that

$$\begin{aligned} [H, \gamma_n] &= -\epsilon_n \gamma_n \\ [H, \gamma_n^\dagger] &= \epsilon_n \gamma_n^\dagger \end{aligned} \tag{18}$$

To be consistent with [7], we define the Nambu vector $\Psi(\vec{r})$ as $\Psi(\vec{r}) = (u_\uparrow(\vec{r}), u_\downarrow(\vec{r}), v_\downarrow(\vec{r}), v_\uparrow(\vec{r}))^T$. Calculating $[H, \psi_\sigma]$ from (15), substituting (17) and (18), and assuming that $\{\gamma_n\}$ form an orthogonal basis, we arrive at the following equation for $\Psi(\vec{r})$.

$$\begin{pmatrix} H_e & W & 0 & \hat{\Delta} \\ W^\dagger & H_e & \hat{\Delta} & 0 \\ 0 & \hat{\Delta}^\dagger & -H_e & W^\dagger \\ \hat{\Delta}^\dagger & 0 & W & -H_e \end{pmatrix} \cdot \Psi(\vec{r}) = H_{BdG}(z) \cdot \Psi(\vec{r}) = \epsilon \Psi(\vec{r}) \tag{19}$$

where $H_e \doteq \frac{P^2}{2m_e} - \mu + Vd\delta(z)$, $W \doteq -\frac{\Delta_{xc}}{2}\Theta(-z) + \frac{\lambda}{\hbar}(P_y + iP_x)\delta(z)$ and $\Delta' \doteq \Delta\Theta(z)$. The matrix operator in the above expression is called the *Bogoliubov-de Gennes Hamiltonian*.

3.3 Calculation of the transmission coefficients

Here we use the scattering matrix formalism in the calculation of the transmission coefficient [7]. If we consider an electron excitation coming from the

F side, with spin σ, and satisfying eq. (19), the possible scattering processes are only those shown in figure 5.

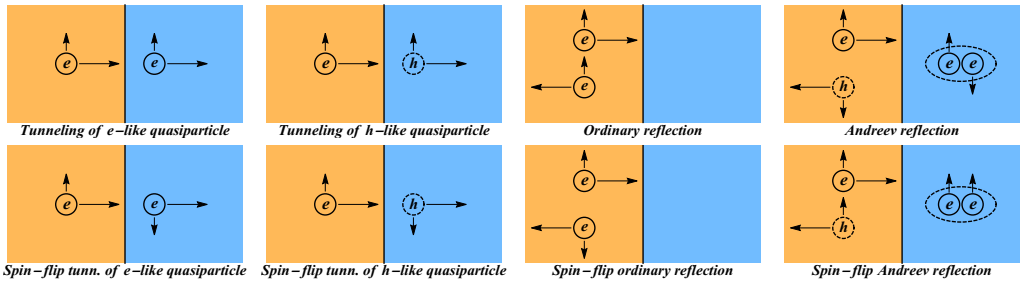

Figure 5: Possible scattering events for an incoming electron from the F side. The Andreev reflection and its spin-flip counterpart correspond to a process where the incoming electron couples with another electron at the junction, forming a Cooper pair in the superconductor and leaving a hole on the F side.

Since the parallel wave-vector $\vec{k}_{\parallel}$ of the incoming electron is conserved in all scattering events, we look for a solution to (19) of the form

$$\Psi(\vec{r}) = \Psi(z)e^{i\vec{k}_{\parallel}\cdot\vec{r}_{\parallel}}, \tag{20}$$

and to be consistent with the possible scattering events, in the F region $\Psi(z)$ must be given by:

$$\Psi^F_\sigma(z) = \frac{1}{\sqrt{k^e_\sigma}} \begin{pmatrix} \frac{\sigma}{\sqrt{2}} \\ \frac{1}{\sqrt{2}} \\ 0 \\ 0 \end{pmatrix} e^{ik^e_\sigma z} + r^e_{\sigma,\sigma} \begin{pmatrix} \frac{\sigma}{\sqrt{2}} \\ \frac{1}{\sqrt{2}} \\ 0 \\ 0 \end{pmatrix} e^{-ik^e_\sigma z} + r^e_{\sigma,-\sigma} \begin{pmatrix} \frac{-\sigma}{\sqrt{2}} \\ \frac{1}{\sqrt{2}} \\ 0 \\ 0 \end{pmatrix} e^{-ik^e_{-\sigma} z} \tag{21}$$

$$+ r^h_{\sigma,\sigma} \begin{pmatrix} 0 \\ 0 \\ \frac{-\sigma}{\sqrt{2}} \\ \frac{1}{\sqrt{2}} \end{pmatrix} e^{ik^h_\sigma z} + r^h_{\sigma,-\sigma} \begin{pmatrix} 0 \\ 0 \\ \frac{\sigma}{\sqrt{2}} \\ \frac{1}{\sqrt{2}} \end{pmatrix} e^{ik^h_{-\sigma} z},$$

and in the S region, by:

$$\Psi_\sigma^S(z) = t^e_{\sigma,\sigma}\begin{pmatrix}u\\0\\v\\0\end{pmatrix}e^{iq^e z}+t^e_{\sigma,-\sigma}\begin{pmatrix}0\\u\\0\\v\end{pmatrix}e^{iq^e z}+t^h_{\sigma,\sigma}\begin{pmatrix}v\\0\\u\\0\end{pmatrix}e^{-iq^h z}+t^h_{\sigma,-\sigma}\begin{pmatrix}0\\v\\0\\u\end{pmatrix}e^{-iq^h z}, \tag{22}$$

where

$$k_\sigma^{e(h)} = \sqrt{k_F^2 - k_\parallel^2 + \frac{2m}{\hbar^2}\left(\sigma\frac{\Delta_{xc}}{2} + (-)E\right)},$$
$$q^{e(h)} = \sqrt{k_F^2 - k_\parallel^2 + (-)\frac{2m}{\hbar^2}\sqrt{E^2-\Delta^2}},$$
$$u(v) = \sqrt{\frac{1+(-)\sqrt{1-\frac{\Delta^2}{E^2}}}{2}}, \quad k_F = \frac{\sqrt{2m\mu}}{\hbar} \quad \text{and} \quad \sigma = \pm 1.$$

The first term of (21) corresponds to the incoming electron. The coefficients $r^e_{\sigma,\sigma}$, $r^e_{\sigma,-\sigma}$, $r^h_{\sigma,-\sigma}$, $r^h_{\sigma,\sigma}$ correspond to the processes of ordinary reflection, spin-flip reflection, Andreev reflection, and spin-flip Andreev reflection, respectively, and $t^e_{\sigma,\sigma}$, $t^e_{\sigma,-\sigma}$, $t^h_{\sigma,\sigma}$, $t^h_{\sigma,-\sigma}$ correspond to the processes of electron-like tunneling, spin-flip electron-like tunneling, hole-like tunneling and spin-flip hole-like tunneling, respectively.

To obtain the scattering coefficients, we must solve the linear system obtained by applying the boundary conditions: the continuity of the wave-function at the boundary, and the discontinuity of its derivative, due to the boundary interactions

$$\Psi_\sigma^F|_{z=0^+} = \Psi_\sigma^S|_{z=0^-} \tag{23}$$

$$\frac{\hbar^2}{2m}\left(\frac{d}{dz}\Psi_\sigma^S|_{z=0^-} - \frac{d}{dz}\zeta\Psi_\sigma^F|_{z=0^+}\right) = Vd\zeta\Psi_\sigma^F|_{z=0^+} + \begin{pmatrix}\vec{\lambda}\cdot\hat{\sigma} & 0\\ 0 & -\vec{\lambda}\cdot\hat{\sigma}\end{pmatrix}\Psi_\sigma^F|_{z=0^+},$$

where $\zeta = diag(1,1,-1,-1)$. From the scattering coefficients, we define the reflection coefficients [4]

$$R_\sigma^{e(h)}(E,k_\parallel) = Re[k_\sigma^{e(h)}|r_{\sigma,\sigma}^{e(h)}|^2 + k_{-\sigma}^{e(h)}|r_{\sigma,-\sigma}^{e(h)}|^2].$$

$R_\sigma^{e(h)}(E, k_\parallel)$ corresponds to the reflection coefficient of an electron (hole), for an incoming electron with energy E, parallel wave-vector $k_\parallel$ and spin σ. Finally, the transmission coefficient over the FS junction is given by

$$\mathcal{T}(E) = \sum_\sigma \int [1 + R_\sigma^h\left(E, k_\parallel\right) - R_\sigma^e\left(E, k_\parallel\right)] d^2 k_\parallel. \tag{24}$$

3.4 Calculation of the pairing amplitude

The pairing amplitude is defined as

$$\begin{aligned} F_{\alpha,\beta}(\vec{r}, t) &\doteq \langle \mathcal{T} \psi_\alpha(\vec{r}, t) \psi_\beta(\vec{r}, 0) \rangle \\ &= \Theta(t) \langle \psi_\alpha(\vec{r}, t) \psi_\beta(\vec{r}, 0) \rangle - \Theta(-t) \langle \psi_\beta(\vec{r}, 0) \psi_\alpha(\vec{r}, t) \rangle \end{aligned} \tag{25}$$

In the Heisenberg picture, we have $\psi_\sigma(\vec{r}, t) = e^{Ht} \psi_\sigma(\vec{r}, 0) e^{-iHt}$, and $\gamma_n(t) = e^{iHt} \gamma_n(0) e^{-iHt}$. Moreover, the equation of motion for γ_n is given by

$$i\hbar \frac{d}{dt} \gamma_n(t) = [\gamma_n(t), H] = \epsilon_n \gamma_n(t) \quad \Rightarrow \quad \gamma_n(t) = e^{-i\frac{\epsilon_n}{\hbar} t} \gamma_n(0) \tag{26}$$

Therefore, from (17), we find that

$$\begin{aligned} \psi_\uparrow(\vec{r}, t) &= \sum_n (u_{n\uparrow}(\vec{r}) \gamma_n(0) e^{-i\epsilon_n t} - v_{n\uparrow}^*(\vec{r}) \gamma_n^\dagger(0) e^{i\epsilon_n t}) \\ \psi_\downarrow(\vec{r}, t) &= \sum_n (u_{n\downarrow}(\vec{r}) \gamma_n(0) e^{-i\epsilon_n t} + v_{n\downarrow}^*(\vec{r}) \gamma_n^\dagger(0) e^{i\epsilon_n t}) \end{aligned} \tag{27}$$

We assume that our system system is on its ground state, which corresponds to the vacuum state of the operators $\{\gamma_n\}$ (see eq. (16)). Hence, using (27) we can compute the expected values in (25). Along the $\hat{z}$ direction, the pairing amplitudes are given by [6]

$$
\begin{aligned}
F_{\uparrow\uparrow}(z,t) &= -\sum_n \left(\Theta(t)u_{n\uparrow}(z)v^*_{n\uparrow}(z)e^{-i\frac{\epsilon_n}{\hbar}t} - \Theta(-t)u_{n\uparrow}(z)v^*_{n\uparrow}(z)e^{i\frac{\epsilon_n}{\hbar}t}\right) \\
F_{\downarrow\downarrow}(z,t) &= \sum_n \left(\Theta(t)u_{n\downarrow}(z)v^*_{n\downarrow}(z)e^{-i\frac{\epsilon_n}{\hbar}t} - \Theta(-t)u_{n\downarrow}(z)v^*_{n\downarrow}(z)e^{i\frac{\epsilon_n}{\hbar}t}\right) \\
F_{\uparrow\downarrow}(z,t) &= \sum_n \left(\Theta(t)u_{n\uparrow}(z)v^*_{n\downarrow}(z)e^{-i\frac{\epsilon_n}{\hbar}t} + \Theta(-t)u_{n\downarrow}(z)v^*_{n\uparrow}(z)e^{i\frac{\epsilon_n}{\hbar}t}\right) \\
F_{\downarrow\uparrow}(z,t) &= -\sum_n \left(\Theta(t)u_{n\downarrow}(z)v^*_{n\uparrow}(z)e^{-i\frac{\epsilon_n}{\hbar}t} + \Theta(-t)u_{n\uparrow}(z)v^*_{n\downarrow}(z)e^{i\frac{\epsilon_n}{\hbar}t}\right)
\end{aligned}
\tag{28}
$$

To compute the Fourier transform of the pairing amplitudes, we must add a convergence factor $e^{-\delta|t|}$:

$$
\tilde{F}_{\alpha,\beta}(\vec{r},\omega) = \lim_{\delta\to 0^+}\int_{-\infty}^{\infty} F_{\alpha,\beta}(\vec{r},t)e^{i\omega t}e^{-\delta|t|}dt \tag{29}
$$

Again on the $\hat{z}$ direction, we have

$$
\begin{aligned}
\tilde{F}_{\uparrow\uparrow}(z,\omega;\delta) &= -i\sum_{n=-\infty}^{\infty}\frac{u_{n\uparrow}(z)v^*_{n\uparrow}(z)}{\omega-\epsilon_n+i\delta_n} \\
\tilde{F}_{\downarrow\downarrow}(z,\omega;\delta) &= i\sum_{n=-\infty}^{\infty}\frac{u_{n\downarrow}(z)v^*_{n\downarrow}(z)}{\omega-\epsilon_n+i\delta_n} \\
\tilde{F}_{\uparrow\downarrow}(z,\omega;\delta) &= i\sum_{n=-\infty}^{\infty}\frac{u_{n\uparrow}(z)v^*_{n\downarrow}(z)}{\omega-\epsilon_n+i\delta_n} \\
\tilde{F}_{\downarrow\uparrow}(z,\omega;\delta) &= -i\sum_{n=-\infty}^{\infty}\frac{u_{n\downarrow}(z)v^*_{n\uparrow}(z)}{\omega-\epsilon_n+i\delta_n}
\end{aligned}
\tag{30}
$$

where $\delta_n = \delta$ if $\epsilon_n > 0$ and $-\delta$ if $\epsilon_n < 0$. Since ϵ_n and $(u_{n\uparrow}(z), u_{n\downarrow}(z), v_{n\uparrow}(z), v_{n\downarrow}(z))^T$ are, respectively, eigenvalues and eigenvectors of $H_{BdG}(z)$, the pairing amplitudes above can be related with the inverse of $H_{BdG}(z)$. In fact, the Green's function

$$
G(z,\omega) \doteq (H_{BdG}(z) - \omega\mathbb{1})^{-1} \tag{31}
$$

can be written as

$$G(z,\omega) = \begin{pmatrix} G_{ee}(z,\omega) & G_{eh}(z,\omega) \\ G_{he}(z,\omega) & G_{hh}(z,\omega) \end{pmatrix} \tag{32}$$

where

$$G_{eh}(z,\omega) = \begin{pmatrix} \tilde{F}_{\uparrow\uparrow}(z,\omega) & \tilde{F}_{\uparrow\downarrow}(z,\omega) \\ \tilde{F}_{\downarrow\uparrow}(z,\omega) & \tilde{F}_{\downarrow\downarrow}(z,\omega) \end{pmatrix} \tag{33}$$

Hence, the pairing amplitudes can be obtained by computing the matrix elements of the Green's function G.

In order to compute the odd-frequency pairing amplitude in our junction, first we discretize the system in the z direction [1], and take the inverse-FT of the wave-vectors $u_\alpha(\vec{r}), v_\alpha(\vec{r})$ in the x and y coordinates, as our system is translational-invariant with respect to those directions.

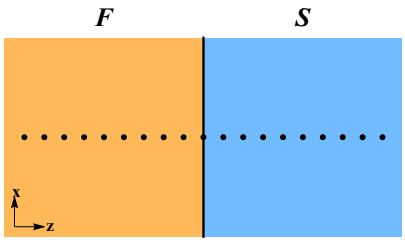

Figure 6: Representation of the discretized system. The dots represent the lattice sites along the z direction.

Then, we can write the matrix elements of BdG Hamiltonian in the z direction, and calculate $G(z,\omega)$ by (31). In our simulations, we discretized the system in 101 lattices: 50 lattices for the ferromagnet side, 50 lattices for the superconductor side, and 1 lattice for the junction. The results were also computed using the following variables (see table 1).

Z	Barrier strength	$\frac{Vdm}{\hbar^2 k_F}$
Λ	Rashba field strength	$\frac{2\lambda m}{\hbar^2}$
P	Spin polarization	$\frac{\Delta_{xc}}{2\mu}$

Table 1: Normalized variables used in the simulations. Z is related to the barrier strength, Λ to the Rashba interaction strength, and P is the degree of polarization.

4 Results

4.1 Superconducting pairing amplitude

In Fig. 7 we show the behavior of the pairing amplitude as a function of ω for the discretized system. We present all the four spin configurations, spin-singlet and the three different types of spin-triplets. We see that both the equal-spin and mixed-spin triplet pairings are odd functions of ω whereas the spin-singlet pairing is even. Both real and imaginary parts of the pairing functions satisfy this condition. This phenomenon can be explained by the Fermi-Dirac statistics of the electrons of the Cooper pair. We show the results for a single site of the ferromagnet, but it is true for all other sites.

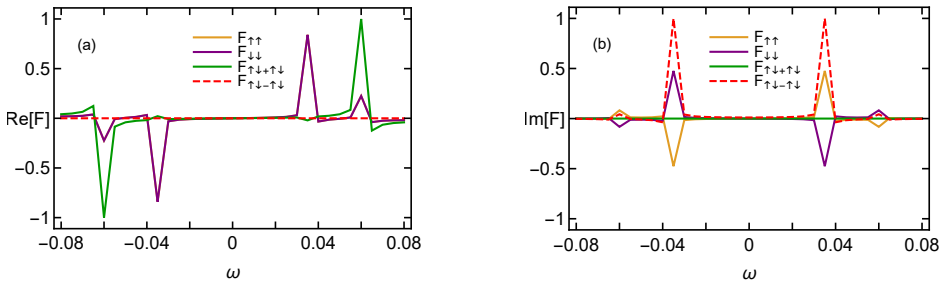

Figure 7: (a) Real and (b) imaginary parts of the pairing amplitude $\mathcal{F}$ as a function of the frequency ω, for $Z = 0, \Lambda = 0.3$ and $P = 0.4$. The superconducting gap Δ is taken to be 0.5.

Now we plot the pairing amplitude at different sites of the ferromagnet for various values of the polarization and the Rashba strength in Fig. 8. The upper and the lower panel correspond to $\Lambda = 0$ and $\Lambda = 1$, respectively. We observe that, $(8(a), (b)$, and $(c))$, the proximity-induced spin-singlet pairing amplitude (dashed line) decreases as P increases in absence of Rashba field. It happens because the polarization of the ferromagnet tends to align the spins, thus breaking the spin-singlet pairing. Note that we set the polarization of the ferromagnet along the x axis, that means, parallel to the plane of the junction. However, when $\Lambda \neq 0$ $(8(d), (e)$, and $(f))$, when we increase the polarization, the amplitude of all the spin-triplet pairings (solid line) increases, whereas the spin-singlet pairing decays similar to the previous case. In presence of Rashba field, whenever we are increasing the polarization, the asymmetry in the spin density of states in the ferromagnet increases. For

$P = 1$, we have only one spin band in the ferromagnet. Therefore, with the increase of the polarization, ordinary Andreev reflection associated with the proximity induced superconductivity decreases. The presence of Rashba field at the junction causes sin-flip Andreev reflection and we have spin-triplet pairing amplitude. On the whole, the behaviour of the proximity-induced pairing amplitude is oscillatory within the ferromagnet. Therefore, only spin-triplet odd-frequency pairing is present in the system when the ferromagnet is in the half-metal regime; that means, $P \approx 1$, in presence of finite Rashba field.

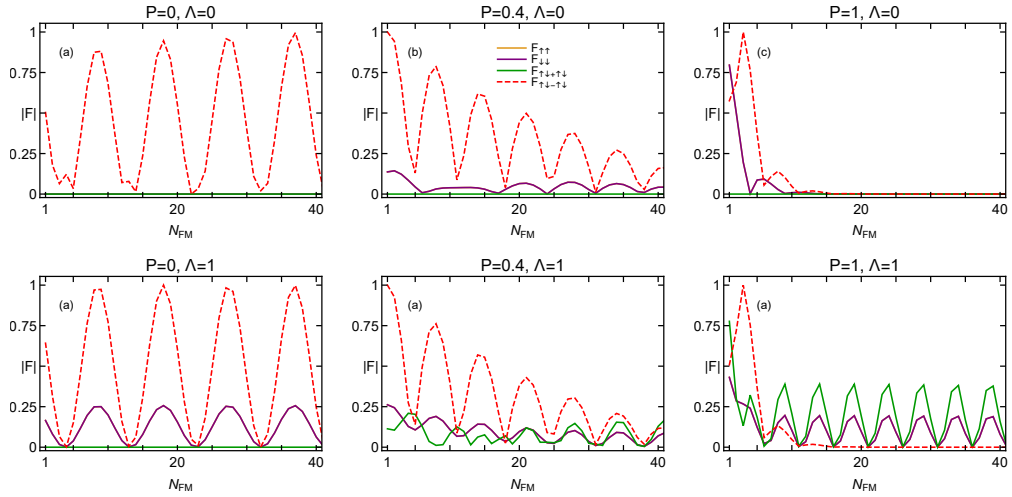

Figure 8: Behavior of the normalized pairing amplitude for different polarizations and Rashba field strength, assuming $Z = 0$ and $\Delta = 0.5$. The x axis corresponds to the lattice sites inside the ferromagnet. The junction is at $N = 0$, and for each case, ω was taken to be one half the energy of the first excited state (generally ~ 0.01).

4.2 Thermoelectric coefficients

Fig. 8 shows that for high P and in presence of a nonzero Rashba interaction, odd-frequency triplet pairing amplitudes dominate over the singlet pairing. Now we show the Seebeck coefficient and the thermoelectric figure of merit of our FS junction (see figures 9 and 10). In our simulations, we assume a temperature-dependent gap given by $\frac{\Delta(T)}{\Delta(0)} = \tanh\left(\sqrt{\frac{T_c}{T} - 1}\right)$, where T_c is the critical temperature for superconductivity. In the simulations, we take $T/T_c = 0.5$, and ignore terms of the order $\frac{E}{\mu}$, as $\mu >> 1$ and only excitations

with energy close to 0 are relevant (this is approximation also known as *Andreev apppoximation*).

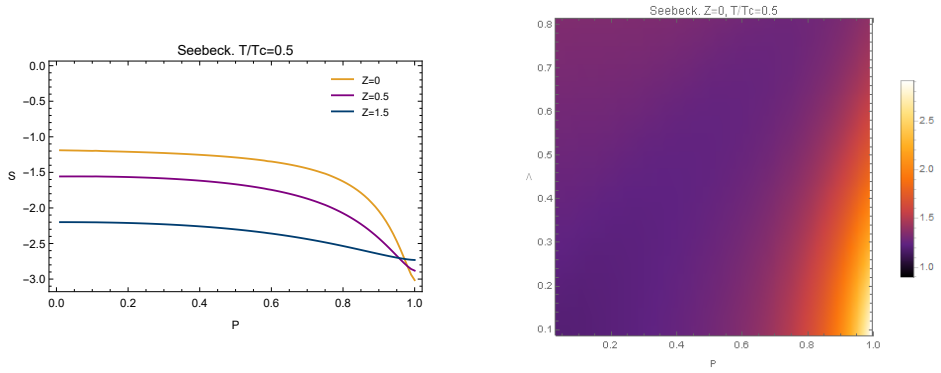

Figure 9: Left: Seebeck coefficient as a function of the polarization for different barrier strengths and $\Lambda = 0$. Right: Density plot of the absolute value of Seebeck coefficient as a function of polarization and Rashba field.

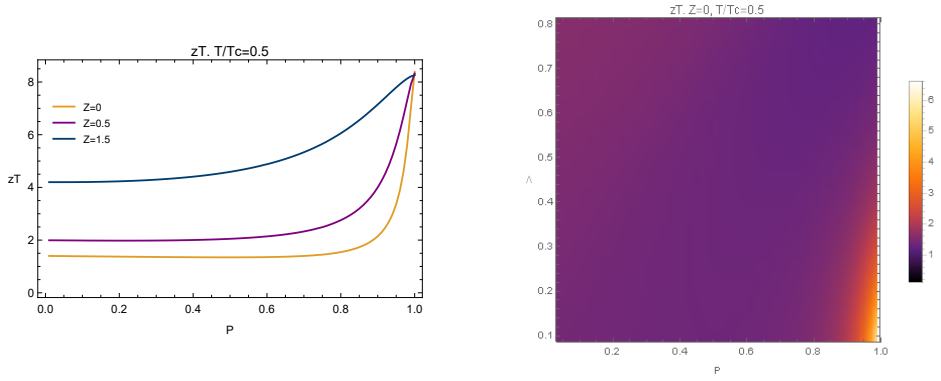

Figure 10: Left: zT coefficient as a function of the polarization for different barrier strengths and $\Lambda = 0$. Right: Density plot of the absolute value of zT coefficient as a function of polarization and Rashba field.

We see that for $P \simeq 1$ and small Λ there is an enhancement of S and zT (see figures 9 and 10), when we have only odd-frequency pairing in the system. It is true for all barrier strength.

To see whether this enhancement is due to the odd-frequency spin-triplet pairings, we look at the contributions only from the sug-gap energy levels; that is, $E \leq \Delta$, in Fig. 11. In this regime, the only scattering processes that

contributes to the enhancement of the thermal coefficients are the Andreev processes, since tunneling is forbidden for excitations with $E < \Delta$. However, since for $P \approx 1$ the singlet pairing amplitude is suppressed, and only spin-flip Andreev reflection is possible, the contribution of the sub-gap regime measures also the contribution of odd-frequency superconductivity in the values of the thermal coefficients.

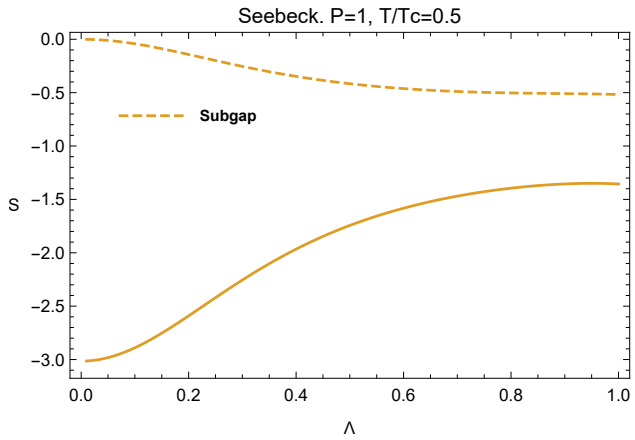

Figure 11: Plot of the Seebeck coefficient for $P = 1$ (solid line) and the sub-gap contribution (dashed line). As Λ grows, the sub-gap contribution increases.

Fig. 11 shows that, for $P = 1$, as we increase Λ, the sub-gap contribution to the Seebeck coefficient also increases, as spin-flip Andreev reflection becomes more probable, and so raising the triplet pairing amplitude. We see that, for $T/T_c = 0.5$ and $\Lambda \approx 0.8$, we have a major contribution from the sub-gap regime.

5 Conclusion

From the above calculations, it can be concluded that in the half-metallic regime ($P \simeq 1$) and in presence of a Rashba interaction, the odd-frequency superconductivity dominates over the even-frequency superconductivity. This happens due to the the spin-flip Andreev reflection scattering process, and it is responsible for a major sub-gap contribution of the thermal coefficients. Hence, measuring the thermal coefficients in a FS junction under such conditions is an indirect way of probing odd-frequency superconductivity in the system. Moreover, as S and zT are greater than 1 in the regime studied, this indicates that odd-frequency based materials might be good thermoelectrics.

References

[1] Yasuhiro Asano, Yukio Tanaka, and Alexander A Golubov. Josephson effect due to odd-frequency pairs in diffusive half metals. *Physical review letters*, 98(10):107002, 2007.

[2] John Bardeen, Leon N Cooper, and John Robert Schrieffer. Theory of superconductivity. *Physical review*, 108(5):1175, 1957.

[3] V. L. Berezinskii. New model of the anisotropic phase of superfluid he3. *Pisma Zh. Eksp. Teor. Fiz.*, 20:628, 1974.

[4] Paramita Dutta, Arijit Saha, and AM Jayannavar. Thermoelectric properties of a ferromagnet-superconductor hybrid junction: Role of interfacial rashba spin-orbit interaction. *Physical Review B*, 96(11):115404, 2017.

[5] Matthias Eschrig and Tomas Löfwander. Triplet supercurrents in clean and disordered half-metallic ferromagnets. *Nature Physics*, 4(2):138, 2008.

[6] Klaus Halterman, Oriol T Valls, and Paul H Barsic. Induced triplet pairing in clean s-wave superconductor/ferromagnet layered structures. *Physical Review B*, 77(17):174511, 2008.

[7] Petra Högl, Alex Matos-Abiague, Igor Žutić, and Jaroslav Fabian. Magnetoanisotropic andreev reflection in ferromagnet-superconductor junctions. *Physical review letters*, 115(11):116601, 2015.

[8] Sun-Yong Hwang, Pablo Burset, and Björn Sothmann. Odd-frequency superconductivity revealed by thermopower. *Physical Review B*, 98(16):161408, 2018.

[9] Abram Fedorovich Ioffe. *Physics of semiconductors*. Infosearch, 1960.

[10] Jacob Linder and Alexander V Balatsky. Odd-frequency superconductivity. *arXiv preprint arXiv:1709.03986*, 2017.

[11] Jacob Linder and Alexander V. Balatsky. Odd-frequency superconductivity. *arXiv e-prints*, page arXiv:1709.03986, Sep 2017.

[12] Lars Onsager. Reciprocal relations in irreversible processes. i. *Physical review*, 37(4):405, 1931.

[13] Lars Onsager. Reciprocal relations in irreversible processes. ii. *Physical review*, 38(12):2265, 1931.